

Accuracy versus Predominance: Reassessing the validity of the quasi-steady-state approximation

Kashvi Srivastava^a, Justin Eilertsen^b, Victoria Booth^a, Santiago Schnell^c

^a*Department of Mathematics, University of Michigan, Ann Arbor, MI 48109, USA*

^b*Mathematical Reviews, American Mathematical Society, 416 4th Street, Ann Arbor, MI 48103, USA*

^c*Department of Biological Sciences and Department of Applied & Computational Mathematics & Statistics, University of Notre Dame, Notre Dame, IN 46556, USA*

Abstract

The application of the standard quasi-steady-state approximation to the Michaelis–Menten reaction mechanism is a textbook example of biochemical model reduction, derived using singular perturbation theory. However, determining the specific biochemical conditions that dictate the validity of the standard quasi-steady-state approximation remains a challenging endeavor. Emerging research suggests that the accuracy of the standard quasi-steady-state approximation improves as the ratio of the initial enzyme concentration, e_0 , to the Michaelis constant, K_M , decreases. In this work, we examine this ratio and its implications for the accuracy and validity of the standard quasi-steady-state approximation. Using standard tools from the analysis of ordinary differential equations, we show that while e_0/K_M provides an indication of the standard quasi-steady-state approximation’s asymptotic accuracy, the sQSSA’s predominance relies on a small ratio of e_0 to the Van Slyke-Cullen constant, K . We conclude that the magnitude of e_0/K offers the most accurate measure of the validity of the standard quasi-steady-state approximation.

Keywords: Singular perturbation, quasi-steady-state approximation, Michaelis–Menten reaction mechanism, timescale separation

1. Introduction

The Michaelis–Menten (MM) reaction mechanism, a cornerstone of enzyme kinetics, describes the irreversible catalysis of a substrate, S , into product, P , by an enzyme, E :



where C represents an enzyme-substrate intermediate complex [1]. The simplest form of the mass action equations modeling the dynamics of the substrate, complex, enzyme, and product concentrations (s , c , e , and p , respectively) is a two-dimensional system of ordinary

Email address: santiago.schnell@nd.edu (Santiago Schnell)

differential equations (ODEs):

$$\dot{s} = -k_1(e_0 - c)s + k_{-1}c, \quad (2a)$$

$$\dot{c} = k_1(e_0 - c)s - (k_{-1} + k_2)c, \quad (2b)$$

with $\dot{e} = -\dot{c}$, $\dot{p} = k_2c$, where “ $\dot{\cdot}$ ” denotes differentiation with respect to time, t . The constant, e_0 , is the initial enzyme concentration, a conserved quantity.

Closed-form solutions to (2) are unattainable due to quadratic nonlinearities. Consequently, reduced equations approximating the long-time dynamics of (2) are often employed to both elucidate the kinetics of (1) and serve as a forward model for parameter estimation from in vitro progress curve experiments via nonlinear regression [2, 3, 4]. The standard quasi-steady-state approximation (sQSSA) to the mass action equations associated with the MM reaction mechanism is a well-known and extensively studied reduced model in biochemical kinetics [2, 5]. Simply put, the sQSSA is a differential algebraic equation (DAE) that approximates the depletion of substrate:

$$\dot{s} = -\frac{k_2e_0s}{K_M + s}, \quad c = \frac{e_0s}{K_M + s} \quad (3)$$

where $K_M = (k_{-1} + k_2)/k_1$ is the Michaelis constant and k_2e_0 is the limiting rate. The Michaelis constant is composite of the equilibrium constant $K_S = k_{-1}/k_1$ and the Van Slyke-Cullen constant $K = k_2/k_1$, and can be expressed as $K_M = K_S + K$. We assume initial conditions for (2) lie on the s -axis, i.e., $(s, c)(0) = (s_0, 0)$. Under this assumption, we can equip (3) with the initial condition $s(0) = s_0$.

Geometric singular perturbation theory provides mathematical justification for (3): with $(s, c)(0) = (s_0, 0)$, the solution to mass action system (2) converges to the DAE (3) in the limit as $e_0 \rightarrow 0$, provided all other parameters, k_{-1}, k_2 and k_1 , are bounded above and below by positive constants [see, e.g. 6, 7]. For further information on geometric singular perturbation theory, see Kaper and Kaper [8], Hek [9], Jones [10] and Wechselberger [11].

While the mathematical rationale behind (3) is well-established, applying (3) presents a challenge: determining how small e_0 must be to ensure (3) is sufficiently accurate. This assessment is complicated by the relative nature of “small.” e_0 is only small compared to another quantity, but what is that quantity? Emerging research [see, e.g. 12, 13, 7] suggests that the sQSSA is accurate whenever $e_0 \ll K_M$, or $\varepsilon_{RS} = e_0/K_M \ll 1$, which we refer to as the Reich-Sel’kov condition [14]. Thus, the “other” quantity is the Michaelis constant, K_M , and the sQSSA is considered *valid* – in the sense of accuracy – when the Reich-Sel’kov condition holds.

Beyond accuracy, it is crucial to determine conditions that ensure the *predominance* of the sQSSA (3). When the reaction unfolds away from the singular limit (i.e., with $0 < e_0$), multiple reduced models may be accurate. However, it is not obvious that the Reich-Sel’kov condition guarantees that the sQSSA is the predominant reduction. Other reduced models may be more accurate¹ than the sQSSA even when $e_0 \ll K_M$ (see Section 2). Therefore,

¹In this context, *accuracy* refers to the ability of the reduction to approximate the flow on the slow manifold. We are choosing to ignore errors that arise in the approach to the slow manifold.

identifying the most accurate approximation among the available reduced models is essential, and this most accurate model should be labeled as the predominant reduction.

This paper aims to deepen our understanding of the Reich-Sel'kov condition and distinguish between accuracy and predominance concerning the sQSSA (3). To our knowledge, this distinction has not been previously addressed in the literature. Using rigorous phase-plane analysis and methods from ODE analysis, we demonstrate that while the Reich-Sel'kov condition provides a general indication of the sQSSA's accuracy, it does not ensure its predominance, which requires a more restrictive criterion. We derive this qualifier and challenge the notion that the validity of the sQSSA solely pertains to its accuracy. We argue that validity should encompass both the accuracy and predominance of the sQSSA. In essence, the qualifier establishing the sQSSA's validity is more restrictive than any previously reported condition.

2. Fenichel Theory, TFPV Theory, and Literature Review

This section reviews Fenichel theory and Tikhonov-Fenichel Parameter Value (TFPV) theory, placing the problem within a precise mathematical context. We also examine recent literature on the validity of the sQSSA (3).

2.1. A brief introduction of Fenichel theory

Geometric singular perturbation theory, also known as Fenichel theory [15, 16], provides the rigorous foundation for deriving the sQSSA. Consider a perturbed dynamical system:

$$\dot{x} = f(x, \varepsilon), \quad f : \mathbb{R}^n \times \mathbb{R} \rightarrow \mathbb{R}^n \quad (4)$$

where $\varepsilon \in \mathbb{R}$ is a small parameter close to zero.² If the set of singularities:

$$S_0 := \{x \in \mathbb{R}^n : f(x, 0) = 0\} \quad (5)$$

is a non-empty k -dimensional submanifold of \mathbb{R}^n where $0 < k < n$, then (4) is *singularly perturbed* [11]. The rank of the Jacobian with respect to x , $D_1 f(x, 0)$, is constant and equal to $n - k$ along S_0 .

2.1.1. Persistence and Flow

A key result from Fenichel theory states that if S_0 is compact and normally hyperbolic – meaning the $n - k$ non-zero eigenvalues of $D_1 f(x, 0)$ are strictly bounded away from the imaginary axis along S_0 – then S_0 persists. This means an invariant manifold, S_0^ε , exists for $\varepsilon \in [0, \varepsilon_0)$. Expressing S_0^ε as a graph over the first “ k ” coordinates of x

$$S_0^\varepsilon := \{(z, y, \varepsilon) \in \mathbb{R}^k \times \mathbb{R}^{n-k} \times \mathbb{R} : y = h(z, \varepsilon)\}, \quad (6)$$

where $x := (z, y)$ and $z \in \mathbb{R}^k$, $y \in \mathbb{R}^{n-k}$, the flow on S_0^ε is given by:

$$\dot{z}_i = f_i(z, h(z, \varepsilon), \varepsilon), \quad 1 \leq i \leq k \quad (7)$$

where the f_i 's are the component functions of f . Equation (7) describes the evolution of k -independent variables. The evolution of the remaining $n - k$ variables depends on the evolution of z :

$$\dot{y} = D_1 h(z, \varepsilon) \dot{z}, \quad D_1 h(z, \varepsilon) \in \mathbb{R}^{(n-k) \times k}. \quad (8)$$

²We assume $f(x, \varepsilon)$ is sufficiently smooth in both arguments.

2.1.2. Critical Manifolds and Stability

In singular perturbation theory, the submanifold S_0 of stationary points is the *critical manifold*. The persistence of a normally hyperbolic S_0 asserts the existence of a normally hyperbolic invariant manifold, S_0^ε , and also the persistence of its stable and unstable manifolds, $W^s(S_0)$ and $W^u(S_0)$. Thus, S_0^ε inherits the stability properties as S_0 .³ If S_0 is normally hyperbolic and attracting, (7) describes the long-time evolution of (4) because trajectories near S_0^ε contract towards it exponentially.

2.1.3. Approximating the Slow Flow

Fenichel’s initial results require explicit knowledge of S_0^ε , which is often unavailable in practice. To address this, Fenichel [16] proposed a method to approximate the flow in S_0^ε without explicitly knowing it. Expanding $f(x, \varepsilon)$ in a Taylor series near $\varepsilon = 0$ gives:

$$\dot{x} = f(x, 0) + \left. \frac{\partial f(x, \varepsilon)}{\partial \varepsilon} \right|_{\varepsilon=0} \cdot \varepsilon + \mathcal{O}(\varepsilon^2) =: f_0(x) + \varepsilon f_1(x) + \mathcal{O}(\varepsilon^2). \quad (9)$$

If S_0 is normally hyperbolic⁴ and attracting, a splitting exists:

$$T_x \mathbb{R}^n \cong \mathbb{R}^n = \ker D_1 f(x, 0) \oplus \text{image } D_1 f(x, 0) \quad (10)$$

for all $x \in S_0$, where $T_x S_0 \cong \ker D_1 f(x, 0)$ for all $x \in S_0$. Projecting the right-hand side of (9) onto $T_x S_0$ approximates the flow on S_0^ε . This projection is achieved using the operator $\pi^s : \mathbb{R}^n \rightarrow \ker D_1 f(x, 0)$; see Goeke and Walcher [17] and Wechselberger [11] for details on the construction of π^s . The resulting n -dimensional dynamical system (with “ k ” independent variables) is:

$$x' = \pi^s f_1(x)|_{x \in S_0} \quad (11)$$

where “ $'$ ” denotes differentiation with respect to the slow timescale, $\tau = \varepsilon t$. The flow on S_0^ε given by (7) converges to (11) as $\varepsilon \rightarrow 0$. Equation (11) is referred to as quasi-steady-state approximation (QSSA) in chemical kinetics.

2.1.4. Convergence and Initial Conditions

Solutions to (4) with initial condition $x(0) = (z, y)(0) = (z_0, y_0)$ generally do not converge to the solution of (11) with initial condition $z(0) = z_0$ unless z_0 is near S_0 , or z and y are slow and fast coordinates. To ensure convergence, (11) usually requires a modified initial “ \hat{z}_0 ”.

2.2. From Theory to Practice: Tikhonov-Fenichel Parameter Values

Traditional methods for putting mass action equations into perturbation form involve scaling and dimensional analysis, which can be unreliable. A more robust approach considers the mass action equations for a general reaction mechanism:

$$\dot{x} = f(x, p), \quad f : \mathbb{R}^n \times \mathbb{R}^m \rightarrow \mathbb{R}^n \quad (12)$$

³Depending on S_0 , S_0^ε will either be attractive $W^u(S_0) = \emptyset \implies W^u(S_0^\varepsilon) = \emptyset$, repulsive $W^s(S_0) = \emptyset \implies W^s(S_0^\varepsilon) = \emptyset$, or will be of saddle type and come equipped with both stable and unstable manifolds

⁴Normal hyperbolicity of S_0 implies the algebraic and geometric multiplicity of $D_1 f(x, 0)$ ’s trivial eigenvalue is equal to k .

where “ p ” represents an m -tuple of parameters. A point p^* in parameter space is a Tikhonov-Fenichel Parameter Value (TFPV) [6, 18] if:

1. The set $S_0 = \{x \in \mathbb{R}^n : f(x, p^*) = 0\}$ is a k -dimensional submanifold of \mathbb{R}^n with $0 < k < n$, and
2. S_0 is normally hyperbolic.

Expanding $f(x, p)$ near p^* in a direction ρ , $p = p^* + \varepsilon\rho$, gives⁵

$$\dot{x} = f(x, p^*) + \varepsilon D_2 f(x, p^*)\rho, \quad (13)$$

which matches the form (11). This highlights the need to specify a path in parameter space for taking the limit as $\varepsilon \rightarrow 0$ and $p \rightarrow p^*$.

For the MM system (2), the parameter space is a subset of $\mathbb{R}_{\geq 0}^4$ with $p = (e_0, k_1, k_{-1}, k_2)^T$. Here, $p^* := (0, k_1, k_{-1}, k_2)^T$ is a TFPV if k_1, k_{-1}, k_2 are bounded by positive constants. When $p = p^*$, the critical manifold, S_0 , is the s -axis, which is normally hyperbolic and attractive.

To put (2) into perturbation form, we define a curve $\ell(\cdot)$ that passes through p^*

$$\ell(\varepsilon) = \begin{pmatrix} 0 \\ k_1 \\ k_{-1} \\ k_2 \end{pmatrix} + \varepsilon \begin{pmatrix} \widehat{e}_0 \\ 0 \\ 0 \\ 0 \end{pmatrix} = p^* + \varepsilon\rho \quad (14)$$

where $e_0 \mapsto \varepsilon\widehat{e}_0$. This effectively equates “ ε ” with e_0 . The perturbation form of (2) for small e_0 is

$$\begin{pmatrix} \dot{s} \\ \dot{c} \end{pmatrix} = \begin{pmatrix} (k_1 s + k_{-1})c \\ -(k_1 s + k_{-1} + k_2)c \end{pmatrix} + \varepsilon\widehat{e}_0 k_1 s \begin{pmatrix} -1 \\ 1 \end{pmatrix} \quad (15)$$

Projecting the right hand side of (15) onto TS_0 yields the sQSSA (3):

$$\begin{pmatrix} \dot{s} \\ \dot{c} \end{pmatrix} = -\frac{\varepsilon\widehat{e}_0 k_2 s}{K_M + s} \begin{pmatrix} 1 \\ 0 \end{pmatrix} \equiv -\frac{k_2 e_0 s}{K_M + s} \begin{pmatrix} 1 \\ 0 \end{pmatrix}. \quad (16)$$

This derivation implies that the flow on S_0^ε converges to (16) as $e_0 \rightarrow 0$, with other parameters fixed and positive. Furthermore, the solution to the first component of (2) also converges to (16) since the initial condition $(s_0, 0) \in S_0$.

Other TFPV values exist for (2). For instance, with $p^* = (e_0, k_1, k_{-1}, 0)^T$, the Fenichel reduction is the slow product QSS reduction:

$$\begin{pmatrix} \dot{s} \\ \dot{c} \end{pmatrix} = -\frac{k_2 e_0 s (K_S + s)}{K_S e_0 + (K_S + s)^2} \begin{pmatrix} 1 \\ \frac{K_S e_0 - K(K_S + s)}{(K_S + s)^2} \end{pmatrix}, \quad (17)$$

This reduction differs from (16) and will be analyzed in Section 4.

⁵The operator D_2 denotes differentiation with respect to the second argument, p .

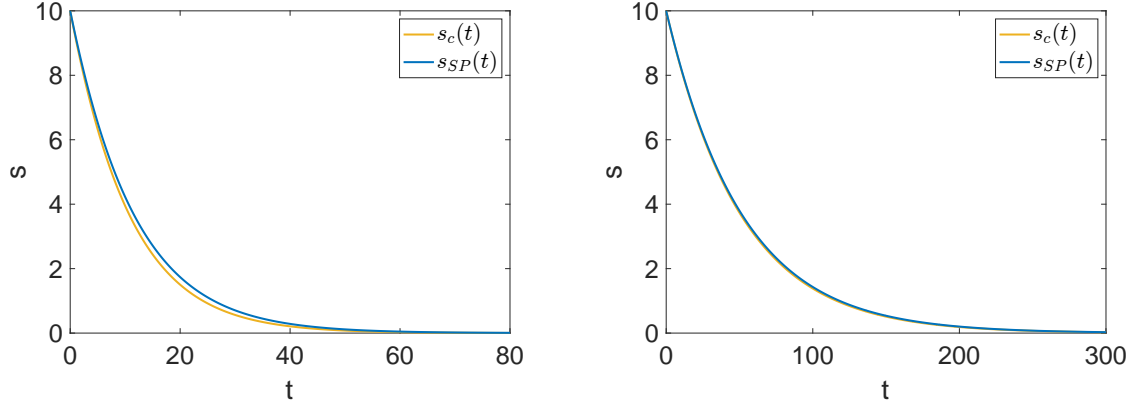


Figure 1: **The sQSSA (16) and the slow product QSSA (17) are indistinguishable for large k_{-1} .** **Left:** $s_0 = 10$, $c_0 = 0$, $e_0 = 10$, $k_1 = 1$, $k_{-1} = 100$, $k_2 = 1$. **Right:** $s_0 = 10$, $c_0 = 0$, $e_0 = 10$, $k_1 = 1$, $k_{-1} = 500$, $k_2 = 1$. Substrate depletion over time is shown in both panels. $s_c(t)$ is the numerical solution to (16) and $s_{SP}(t)$ is the numerical solution to (17).

2.3. The Open Problem: Identifying the Predominant Reduction

Just as important as what Fenichel and TFPV theory tell us is what they do *not*. While the theory indicates that (16) approximates (2) as $e_0 \rightarrow 0$, it does not specify how small e_0 must be for (16) to be valid in practice, where the singular limit is never truly reached. In other words, how small is small enough?

The size of e_0 must be considered relative to other parameters. Fenichel theory requires eigenvalue disparity near the critical manifold. For small e_0 , the ratio of slow and fast eigenvalues near $(s, c) = (0, 0)$ is:

$$\delta := \frac{e_0}{K_M} \cdot \frac{k_2}{k_{-1} + k_2} + \mathcal{O}(e_0^2). \quad (18)$$

While $\delta \ll 1$ is necessary, it is not sufficient for the accuracy of (16) [12]. For instance, consider the case where $e_0 = K_M$ but $k_2 \ll k_{-1}$. This scenario renders small δ , but the tangent vector to the graph of the c -nullcline at the origin will not align with the slow eigenvector, which is crucial for long-time accuracy. This misalignment can lead to significant errors in the sQSSA approximation, even when δ appears to indicate otherwise.

The more restrictive condition $e_0 \ll K_M$, introduced in [14], has been rigorously proven sufficient to guarantee the accuracy of the sQSSA [19, 13, 20, 21, 22]. However, this condition does not fully address the issue of predominance. For instance, if k_{-1} is large and e_0 is reduced such that $k_1 e_0 \ll k_{-1}$ (implying $e_0 \ll K_M$), convergence to (16) is not implied. In fact, as $k_{-1} \rightarrow \infty$, the resulting singular perturbation problem yields a trivial QSSA: $\dot{s} = \dot{c} = 0$ (see Appendix E for the formal calculation).

This example demonstrates that different TFPVs can share a critical manifold and be close in parameter space. For instance, consider a scenario where $k_1 e_0$ and k_2 are relatively small compared to k_{-1} . In this case, the TFPVs $(0, k_1, k_{-1}, k_2)^T$ or $(e_0, k_1, k_{-1}, 0)^T$ could be quite close to each other. Terminating the approach to one TFPV might inadvertently lead to a point in parameter space that is actually closer to another TFPV.

Numerical simulations (FIGURE 1) illustrate this phenomenon. When k_{-1} is significantly large, the trajectories of the system under the sQSSA (16) and the slow product QSSA (17)

become virtually indistinguishable. This makes it challenging to definitively determine which reduction is more accurate or appropriate for the given parameter values.

Moreover, the presence of multiple TFPVs introduces ambiguity in assessing the validity of the sQSSA. For example, if $e_0 = 1$, $k_1 = 0.1$, $k_{-1} = 10$, and $k_2 = 0.1$, it is unclear whether the system's behavior is better approximated by the sQSSA associated with the TFPV $(0, k_1, k_{-1}, k_2)^T$ or the slow product QSSA associated with $(e_0, k_1, k_{-1}, 0)^T$. This ambiguity arises because the parameter values do not fall neatly within the domain of a single TFPV, making it difficult to determine which reduction provides the most accurate representation of the system dynamics. Determining proximity to different TFPVs is challenging due to the different units of the parameters. A dimensionless indicator is needed.

The fact that the magnitude of e_0/K_M alone does not ensure the sQSSA (16) is the *predominant* reduction is a consequence of having to always operate away from the singular limit in a large parameter space. This naturally leads to the question: does there exist a dimensionless parameter whose magnitude not only ensures the accuracy of the sQSSA (3) but also its predominance among other known QSSAs? In other words, can we define a more comprehensive and robust notion of “validity” that encompasses both accuracy and predominance?

3. Anti-funnels and the Slow Invariant Manifold

As discussed in Section 2, a central challenge in applying Fenichel theory to the MM system is the potential ambiguity arising from different TFPVs sharing the same critical manifold. This can lead to uncertainty about the validity of a specific reduction away from the singular limit. To address this, we turn to qualitative methods that allow us to determine the location of the slow manifold, S_0^ε , relative to known curves in the phase-plane. This section introduces the anti-funnel theorem, adapted from Hubbard and West [23] and following the approach of Calder and Siegel [24]. We outline a strategy to determine when the sQSSA (3) is not only accurate but also predominant.

Definition 1. Fences and anti-funnels. Consider the first-order differential equation $y' = f(x, y)$ over the interval $x \in I = [a, b]$ where $a < b \leq \infty$ and “ $'$ ” denotes differentiation with respect to x . Let α and β be continuously-differentiable functions that satisfy

$$\alpha'(x) \leq f(x, \alpha(x)) \text{ and } f(x, \beta(x)) \leq \beta'(x) \tag{19}$$

for all $x \in I$.

- (a) The curve α is a *lower fence* and the curve β is an *upper fence*.
- (b) The lower and upper fences are *strong fences* if the respective inequalities are always strict.
- (c) The set

$$\Gamma := \{(x, y) : x \in I, \beta(x) \leq y \leq \alpha(x)\} \tag{20}$$

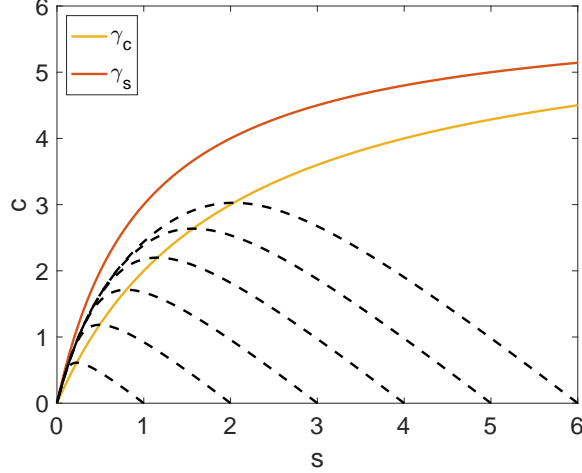


Figure 2: **The region, Γ , between the horizontal nullcline and the vertical nullcline curves is a trapping region on the phase plane.** The numerical solutions to the mass action equations (1) for several initial conditions are denoted by black dashed lines. $s_0 \in \{1, 2, 3, 4, 5, 6\}$, $c_0 = 0$, $e_0 = 6$, $k_1 = 1$, $k_{-1} = 1$, $k_2 = 1$. The numerical solution of trajectories start on the s -axis and eventually enter Γ .

is called an *anti-funnel*⁶ if

$$\beta(x) < \alpha(x) \text{ for all } x \in I.$$

(d) The anti-funnel is *narrowing* if

$$\lim_{x \rightarrow b^-} |\alpha(x) - \beta(x)| = 0. \quad (21)$$

Theorem 1. Anti-funnel Theorem [23]. Consider the first-order differential equation $y' = f(x, y)$ over the interval $I = [a, b)$ where $a < b \leq \infty$. If Γ is an *anti-funnel* with a strong lower fence, α , and a strong upper fence, β , then there exists a solution $y(x)$ to the differential equation such that

$$\beta(x) < y(x) < \alpha(x) \text{ for all } x \in I. \quad (22)$$

Furthermore, if Γ is *narrowing* and $\frac{\partial f}{\partial y}(x, y) \geq 0$ in Γ , then the solution $y(x)$ is unique.

For the MM equations (2), we have:

$$\frac{dc}{ds} = -\frac{e_0 s - (K_M + s)c}{e_0 s - (K_S + s)c} =: f(c, s). \quad (23)$$

The distinguished solution to (23), “ $c = y(s)$ ”, satisfying (22) represents the slow manifold, S_0^c . The challenge lies in finding suitable lower and upper fences, $\alpha(s)$ and $\beta(s)$.

⁶In the (x, y) phase plane, if the upper fence lies above the lower fence, the set between the two fences is known as a *funnel*. Conversely, if the lower fence lies above the upper fence, the set between the two fences is called an *antifunnel* [23]. Refer to [Appendix A](#) for a brief synopsis on the theory of fences and anti-funnels and how it applies to the MM mechanism. See Hubbard and West [23] for the detailed theory.

A natural choice for the upper fence is the c -nullcline, γ_c , given by:

$$\text{Graph}(\gamma_c) = \{(s, c) \in \mathbb{R}^2 : c = e_0 s / (K_M + s)\} \quad (24)$$

Considering the biochemically relevant portion of \mathbb{R}^2 , we focus on $\text{Graph}(\gamma_c) \cap \mathbb{R}_{\geq 0}^2$. This choice is advantageous because it represents the quasi-steady-state variety corresponding to the standard reduction (3), and all phase-plane trajectories starting on the s -axis eventually cross it (see Calder and Siegel [24] and Noethen and Walcher [25] for a proof of this statement).

The set Γ enclosed between the c -nullcline and the s -nullcline, γ_s ,⁷ is positively invariant:

$$\Gamma := \{(s, c) \in \mathbb{R}_{\geq 0}^2 : \gamma_c(s) \leq c \leq \gamma_s(s)\} \quad (25)$$

Once a trajectory enters Γ , it remains within Γ as $t \rightarrow \infty$. (see Calder and Siegel [24] and Noethen and Walcher [25] for a detailed proof). FIGURE 2 illustrates this behavior.

Constructing a suitable lower fence requires more analysis. The stationary point $(s, c) = (0, 0)$ is a node with eigenvalues $\lambda_- < \lambda_+ < 0$:

$$\lambda_{\pm} = \frac{k_1}{2}(K_M + e_0) \left(-1 \pm \sqrt{1 - \frac{4Ke_0}{(K_M + e_0)^2}} \right). \quad (26)$$

Under timescale separation in which

$$\frac{Ke_0}{(K_M + e_0)^2} \ll 1/4, \quad (27)$$

trajectories eventually approach the stationary point along the slow eigenvector, v^+ , spanning the one-dimensional subspace:

$$T_0 S_0^\varepsilon = \text{span}(v^+) = \{(s, c) \in \mathbb{R}^2 : c = ms\}, \quad (28)$$

with slope m :

$$m = \frac{1}{2k_{-1}} \left(-k_{-1} - k_2 + k_1 e_0 + \sqrt{(k_{-1} + k_2 + k_1 e_0)^2 - 4k_1 k_2 e_0} \right). \quad (29)$$

Calder and Siegel [24] leverage this property and define the lower fence:

$$\alpha_{cs}(s) := \frac{me_0 s}{e_0 + ms}, \quad (30)$$

and prove that S_0^ε lies between $\gamma_c(s)$ and $\alpha_{cs}(s)$. Notably, the graph of α_{cs} lies below that of γ_s . By proving that

$$\Gamma_{cs} := \{(s, c) : s \in I, \gamma_c(s) \leq c \leq \alpha_{cs}(s)\} \quad (31)$$

⁷The graph of the s -nullcline is the set $\{(s, c) \in \mathbb{R}^2 : c = e_0 s / (K_S + s)\}$,

is a narrowing anti-funnel,⁸ Calder and Siegel [24] prove that the distinguished slow manifold, S_0^ε , also lies in Γ , the region contained between the c - and s -nullcline.

A key feature of (30) is $\alpha'_{cs}(0) = m$. This leads to highly accurate reduced equation for \dot{s} near the stationary point:⁹

$$\dot{s} = -\frac{e_0 s}{e_0 + m s} \cdot (k_1 e_0 - k_{-1} m). \quad (32)$$

Despite its advantages, this approach has limitations. First, the reduction (32) may be unreliable away from the stationary point, even when $\lambda_- \ll \lambda_+ < 0$ (see Eilertsen et al. [26]). Second, the anti-funnel construction leads to the following:

Proposition 1. For (2) with initial condition $(s, c)(0) = (s_0, 0)$, let $t = t_{\text{cross}}$ be the time the trajectory crosses the upper fence $c = \gamma_c(s)$. Then, the bound

$$-\frac{k_2 e_0 s}{K_M + s} \leq \dot{s} \leq -\frac{e_0 s}{e_0 + m s} \cdot (k_1 e_0 - k_{-1} m) \quad (33)$$

holds for all $t \geq t_{\text{cross}}$.

Proof. Since Γ_{cs} is a narrowing anti-funnel, S_0^ε lies between the graphs of $\alpha_{cs}(s)$ and $\gamma_c(s)$. As S_0^ε is invariant, any trajectory entering Γ_{cs} cannot cross it. Therefore, $\beta(s) \leq c \leq \alpha_{cs}(s)$ holds for all $t \geq t_{\text{cross}}$ since Γ is positively invariant and $\Gamma_{cs} \subset \Gamma$. With $\dot{s} = -k_1 e_0 s + k_1 (K_S + s)c$, it follows that

$$-k_1 e_0 s + k_1 (K_S + s)\gamma_c(s) \leq \dot{s} \leq -k_1 e_0 s + k_1 (K_S + s)\alpha_{cs}(s)$$

proving the assertion. □

While the upper bound in (33) is sharper than $\dot{s} \leq 0$, extracting quantitative information about the sQSSA's accuracy and dimensionless parameters like $\varepsilon_{RS} = e_0/K_M$ from (33) is not straightforward.

The goal is to define an anti-funnel with fences that provide both qualitative and quantitative information about S_0^ε and the error for a given QSSA. By “trapping” S_0^ε between suitable upper and lower fences that form narrowing anti-funnels, we can derive qualifiers that determine the accuracy and predominance of various QSSAs.

4. Trapping the Slow Manifold: The Standard QSSA

As stated in Section 3, our strategy is to construct upper and lower fences that form a narrowing anti-funnel. This raises the question: How do we construct suitable fences? One approach is approximating the slow manifold, S_0^ε , via perturbation expansion

$$S_0^\varepsilon = h_0(s) + \varepsilon h_1(s) + \varepsilon^2 h_2(s) + \mathcal{O}(\varepsilon^2). \quad (34)$$

⁸Calder and Siegel [24] define I as $[a, \infty)$ where $a > 0$ is arbitrary.

⁹The equation is obtained via direct substitution of $c = \alpha_{cs}(s)$ into (2a).

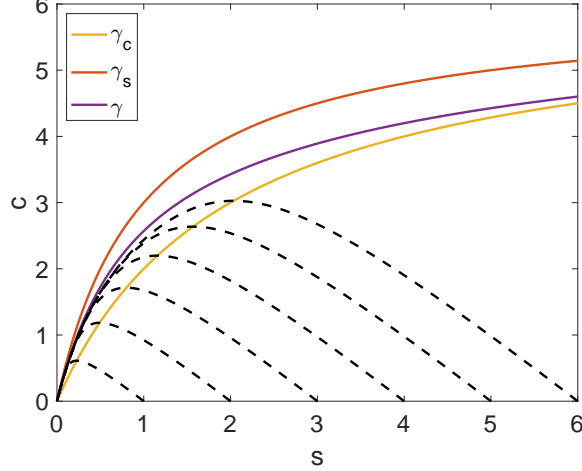


Figure 3: **The region between the horizontal nullcline curve $\gamma_c(s)$ and the curve $\gamma(s)$ is a trapping region on the phase plane.** The numerical solutions to the mass action equations (1) for several initial conditions are denoted by black dashed lines. $s_0 \in \{1, 2, 3, 4, 5, 6\}$, $c_0 = 0$, $e_0 = 6$, $k_1 = 1$, $k_{-1} = 1$, $k_2 = 1$.

Insertion of (34) into the invariance equation results in a *regular* perturbation problem. However, the coefficients in (34) depend on ε , which in turn depends on a specific TFPV. Since we aim for general error bounds, we need fences that are not heavily ε -dependent.

An alternative approach involves combining quantitative reasoning with creative insights. Kumar and Josić [27] sought to approximate the flow on S_0^ε for small k_2 ($k_2 \mapsto \varepsilon \hat{k}_2$). They reasoned that

$$c = \frac{e_0 s}{K_M + s} \quad (35)$$

is a good approximation to S_0^ε when k_2 is small. Under this assumption, the flow of c on S_0^ε is approximately:

$$\dot{c} \approx \frac{d}{ds} \left(\frac{e_0 s}{K_M + s} \right) \dot{s} = \frac{K_M e_0}{(K_M + s)^2} \cdot \dot{s}. \quad (36)$$

Substituting (36) and (35) into the conservation law, $\dot{s} + \dot{c} + k_2 c = 0$, and solving for \dot{s} yields:

$$\dot{s} = - \frac{k_2 e_0 s (K_M + s)}{K_M e_0 + (K_M + s)^2}. \quad (37)$$

This reduction is significant for two reasons. First, it effectively captures the Fenichel reduction for this scenario (compare to (17) with small k_2). Second, the graph of $\gamma(s)$, where

$$\gamma : s \mapsto \frac{e_0 s}{K_S + s} - \frac{k_2 e_0 s (K_M + s)}{k_1 (K_S + s) (K_M e_0 + (K_M + s)^2)}, \quad (38)$$

is an excellent candidate for an appropriate anti-funnel fence.

As shown in Figure 3, γ_c , γ_s and γ are strictly increasing, with $\gamma_c < \gamma < \gamma_s$ for all $s > 0$. The set contained between the graphs of γ_c and γ is positively invariant:

$$\Gamma_0 := \{(s, c) \in \mathbb{R}_{\geq 0}^2 : \gamma_c(s) \leq c \leq \gamma(s)\} \quad (39)$$

Let t_{cross} be the time a trajectory crosses the c -nullcline, as established in [25, 24]. Then, $(s, c)(t) \in \Gamma_0$ for all $t \geq t_{\text{cross}}$. Importantly:

Theorem 2. For the differential equation (23), Γ_0 is a positively invariant, narrowing anti-funnel containing a unique slow manifold, S_0^ε .

Proof. To prove Γ_0 is positively invariant, we show that the vector field for (2) points inwards at the boundary curves:

$$\dot{c}(s, \gamma(s)) - \gamma'(s)\dot{s}(s, \gamma(s)) < 0, \quad (40a)$$

$$\dot{c}(s, \gamma_c(s)) - \gamma_c'(s)\dot{s}(s, \gamma_c(s)) > 0. \quad (40b)$$

See Appendix B for details. Positive invariance implies trajectories entering Γ_0 remain within. Calder and Siegel [24] prove that for solutions initializing on the s -axis, there exists a $t_{\text{cross}} > 0$ at which they enter Γ_0 by crossing γ_c .

From (40), γ and γ_c are strong lower and upper fences, respectively, with $\gamma(s) > \gamma_c(s)$ for $s > 0$. Furthermore,

$$\lim_{s \rightarrow \infty} |\gamma(s) - \gamma_c(s)| = 0 \quad \text{and} \quad \frac{\partial f}{\partial c}(c, s) \geq 0 \quad (41)$$

in Γ_0 . The assertion follows from Theorem 1. \square

Theorem 2 establishes that Γ_0 contains the slow manifold S_0^ε , independent of any specific perturbation scenario. This allows us to extract qualitative and quantitative information about the accuracy of a QSSA and assess predominance when multiple TFPVs are close.

The rest of this section is organized as follows. In Section 4.1, we use the improved trapping region to derive a quantitative error estimate for the sQSS approximation and recover the Reich-Sel'kov condition. In Section 4.2, we explore the conditions where both the sQSS and reverse QSS reductions are valid, examining their validity as we move away from the Reich-Sel'kov condition.

4.1. Accuracy of the Standard QSSA

To leverage Γ_0 's properties, we introduce sharp bounds on the substrate depletion for $t \geq t_{\text{cross}}$, representing the slow regime.

Proposition 2. For system (2) with initial condition $(s, c)(0) = (s_0, 0)$, the bound

$$-\frac{k_2 e_0 s}{K_M + s} \leq \dot{s} \leq -\frac{k_2 e_0 s (K_M + s)}{K_M e_0 + (K_M + s)^2} \quad (42)$$

holds for all $t \geq t_{\text{cross}}$.

Proof. The proof follows from the construction of Γ_0 and substituting $\gamma_c(s) \leq c \leq \gamma(s)$ into (2a). \square

Since the LHS of (42) is the sQSSA for substrate depletion, the design of Γ_0 suggests that the sQSSA performs well when γ and γ_c are close. Rewriting (42) as:

$$-\frac{k_2 e_0 s}{K_M + s} \leq \dot{s} \leq -\frac{k_2 e_0 s}{K_M + s} \left(\frac{1}{1 + \varphi(s)} \right), \quad \varphi(s) = \frac{K_M e_0}{(K_M + s)^2} \quad (43)$$

we see that, for any subinterval $\ell \subset [0, s_0]$,

$$-\frac{k_2 e_0 s}{K_M + s} \leq \dot{s} \leq -\frac{k_2 e_0 s}{K_M + s} \left(\frac{1}{1 + \max_{s \in \ell} \varphi(s)} \right), \quad t_{\text{cross}} \leq t. \quad (44)$$

Since

$$\max_{0 \leq s \leq s_0} \varphi(s) = \frac{e_0}{K_M} = \varepsilon_{RS}, \quad (45)$$

we have:

$$-\frac{k_2 e_0 s}{K_M + s} \leq \dot{s} \leq -\frac{k_2 e_0 s}{K_M + s} \cdot \sum_{j=0}^{\infty} (-1)^j \varepsilon_{RS}^j, \quad t_{\text{cross}} \leq t, \quad \varepsilon_{RS} < 1. \quad (46)$$

This analysis has several significant consequences. First, we have established the sQSSA's asymptotic dependency on ε_{RS} without relying on non-dimensionalization, unlike traditional methods [see 28, 14, 29, among others]. This is advantageous due to the non-uniqueness of non-dimensionalization, which can lead to different “small parameters” [28, 14, 30]. Second, the bound (46) is more aesthetic than the estimate in Eilertsen et al. [13]:

$$-\frac{k_2 e_0 s}{K_M + s} \leq \dot{s} \leq -(1 - m) \frac{k_2 e_0 s}{K_M + s}, \quad t_{\text{cross}} \leq t, \quad (47)$$

where “ m ” is the slope of the slow tangent vector, v^+ .

Third, and this is somewhat unexpected, we gain more information about the approximation error of the flow on S_0^ε from $\varphi(s)$ than from m . From (43), the sQSSA approximates the flow on S_0^ε well in the regions where:

$$K_M e_0 \ll (K_M + s)^2, \quad (48)$$

even if $\varepsilon_{RS} \sim 1$. In particular, the sQSSA is a good approximation in regions where:

$$\max\{K_M, e_0\} \ll s. \quad (49)$$

This relates to the validity of the reverse quasi-steady-state approximation (rQSSA), which operates in high enzyme concentrations. To revisit the sQSSA's predominance, we examine the rQSSA's validity and investigate any overlap in their conditions.

4.2. Validity of the sQSSA for High Enzyme Concentrations

Equation (43) implies that the sQSSA is an excellent approximation to the flow on S_0^ε when $K_M \ll s$ and $e_0 \lesssim s$. In this region, the graphs of the c -nullcline and $\gamma(s)$ approach their horizontal asymptote, $c = e_0$, reflected in $\varphi(s) \rightarrow 0$ as $s \rightarrow \infty$. The slow manifold, S_0^ε , is nearly horizontal implying $\dot{c} \approx 0$ on S_0^ε even for larger ε_{RS} .

Two singular perturbation scenarios lead to a nearly horizontal slow manifold: the sQSSA, where the slow manifold coalesces with the s -axis as $k_1 e_0 \rightarrow 0$, and the rQSSA, coinciding with small k_{-1} and small k_2 :

$$\dot{s} = -k_1(e_0 - c)s + \varepsilon \widehat{k}_{-1}c, \quad (50a)$$

$$\dot{c} = k_1(e_0 - c)s - \varepsilon \widehat{k}_{-1} - \varepsilon \widehat{k}_2. \quad (50b)$$

In the rQSSA scenario, the set of stationary points in the singular limit is not a submanifold of \mathbb{R}^2 :

$$S_0 = S_0^{(1)} \cup S_0^{(2)}$$

where¹⁰

$$S_0^{(1)} = \{(s, c) \in \mathbb{R}_{\geq 0}^2 : s = 0 \text{ \& } 0 \leq c \leq e_0 - \zeta_1\}, \quad 0 < \zeta_1 < e_0, \quad (51a)$$

$$S_0^{(2)} = \{(s, c) \in \mathbb{R}_{\geq 0}^2 : c = e_0 \text{ \& } \zeta_2 \leq s \leq s_0\}, \quad 0 < \zeta_2 < s_0. \quad (51b)$$

Classical Fenichel theory does not apply to the entire set, but it applies to specific compact submanifolds. The resulting Fenichel reduction via projection onto $TS_0^{(2)}$ is:

$$\dot{s} = -k_2 e_0, \quad (52a)$$

$$\dot{c} = 0. \quad (52b)$$

Likewise, the Fenichel reduction obtained via projection onto $TS_0^{(1)}$ is:

$$\dot{s} = 0, \quad (53a)$$

$$\dot{c} = -k_2 c. \quad (53b)$$

In the rQSSA, trajectories initially approach the line $c = e_0$ and stay close until reaching the vicinity of the transcritical bifurcation point, $(s, c) = (0, e_0)$. Near this point, trajectories approach $(0, 0)$ as $t \rightarrow \infty$; however, the slow eigenvector in this scenario is nearly indistinguishable from the c -axis (and in fact aligns with the c -axis in the singular limit).

The rQSSA's long-time validity requires $\varepsilon_{RS}^{-1} \ll 1$, while the sQSSA's long-time validity requires $\varepsilon_{RS} \ll 1$ [19]. However, through comparison, the sQSSA with (52) reveals that they are practically indistinguishable when $K_M \ll e_0 \lesssim s$. Thus, the sQSSA can approximate the flow on S_0^ε to the right of the bifurcation point, extending its validity beyond the Reich-Sel'kov parameter.

A natural question is: If we use the sQSSA to approximate the flow on S_0^ε to the right of the bifurcation instead of (52), how reliable is it in an asymptotic sense? Since S_0^ε lies within Γ_0 when $0 < \varepsilon$, we can get a rough answer. Assuming $\varepsilon_{RS}^{-1} \ll 1$ and considering $s \in [e_0, s_0]$, it follows from (43) that, for $t \geq t_{\text{cross}}$,

$$\begin{aligned} -\frac{k_2 e_0 s}{K_M + s} &\leq \dot{s} \leq -\frac{k_2 e_0 s}{K_M + s} \left(\frac{1}{1 + \max_{s \in [e_0, s_0]} \varphi(s)} \right) \\ &= -\frac{k_2 e_0 s}{K_M + s} \left(\frac{1}{1 + \mu} \right), \quad \mu := \frac{\varepsilon_{RS}}{(1 + \varepsilon_{RS})^2} < \varepsilon_{RS}^{-1} \\ &\leq -\frac{k_2 e_0 s}{K_M + s} \left(\frac{1}{1 + \varepsilon_{RS}^{-1}} \right) \\ &= -\frac{k_2 e_0 s}{K_M + s} \cdot \sum_{j=0}^{\infty} (-1)^j \varepsilon_{RS}^{-j}, \quad 1 < \varepsilon_{RS}. \end{aligned} \quad (54)$$

¹⁰The constants ζ_1, ζ_2 are introduced to enforce the compactness of $S_0^{(1)}$ and $S_0^{(2)}$.

The bound (54) implies the sQSSA is a good approximation when $\varepsilon_{RS}^{-1} \ll 1$ and $e_0 \lesssim s$, improving as $e_0/s \rightarrow 0$.

While the sQSSA approximates the flow on S_0^ε well when $\varepsilon_{RS}^{-1} \ll 1$ and $e_0 \lesssim s$, it cannot be equipped with s_0 as the initial substrate concentration in the rQSSA scenario. If the initial condition is $(s, c)(0) = (s_0, 0)$, with $e_0 < s_0$, Fenichel theory dictates that the reduction (52) should be equipped with $(s, c) = (s_0 - e_0, e_0)$. This extends to the sQSSA if used to approximate the flow on S_0^ε to the right of the bifurcation point when $\varepsilon_{RS}^{-1} \ll 1$.

The existence of multiple accurate QSS reductions under the same conditions necessitates evaluating which QSSA is predominant. To truly verify the standard-QSS reduction's applicability, we must explore other QSS reductions near the sQSS curve in the phase-plane. As noted in Section 3, in scenarios like large k_{-1} , the sQSSA (16) and the slow product QSSA (17) are indistinguishable. To find the most accurate reduced system and its validity conditions, we next investigate the slow manifold's location relative to the (algebraic) variety that generates the slow product QSS reduction (17).

5. Trapping the Slow Manifold: The Slow Product QSSA

This section defines a new upper fence and anti-funnel for the slow manifold using the slow product QSS curve under specific parametric restrictions. We compare this to previous results to assess the approximation accuracy of the sQSSA (16) and the slow product QSSA (17), revisiting the Reich-Sel'kov condition and investigating whether it ensures the predominance of the sQSSA.

The slow product QSS reduction (17), derived from Fenichel theory for small k_2 , corresponds to the QSS curve

$$c = \gamma_{SP}(s) := \frac{e_0 s}{K_S + s} - \frac{k_2 e_0 s}{k_1 (K_S e_0 + (K_S + s)^2)}. \quad (55)$$

This closely resembles the curve $\gamma(s)$. In Section 4.1, we established that the slow manifold lies between $\gamma(s)$ and $\gamma_c(s)$. Now, we explore how the slow product QSS variety fits into these findings and the insights its location provides concerning the sQSSA's validity and predominance.

In the phase plane, $\gamma_{SP}(s)$ lies above the horizontal nullcline $\gamma_c(s)$ for $s < s^*$ where

$$s^* = \frac{k_{-1} e_0}{k_2} - \frac{k_{-1}}{k_1} = \frac{k_{-1}}{k_2} (e_0 - K) \quad (56)$$

is their intersection point for substrate concentration. We are primarily interested in cases where s^* is positive, placing the intersection within the first quadrant. When s^* is negative, or equivalently, when

$$e_0 < K, \quad (57)$$

the slow manifold crosses the sQSS variety, and the sQSSA is the best known reduction.

However, as e_0 increases, s^* shifts to the right. FIGURE 4 shows how the curves' positions change with parameter values. When $e_0 > K$, the intersection point lies in the first quadrant and $\gamma_{SP}(s) \geq \gamma_c(s)$ for $0 \leq s \leq s^*$. Also, $\gamma_{SP}(s) \leq \gamma(s)$ for all $s \geq 0$. Thus, the slow product QSS curve lies within Γ_0 for a significant portion of the phase plane. This raises the questions:

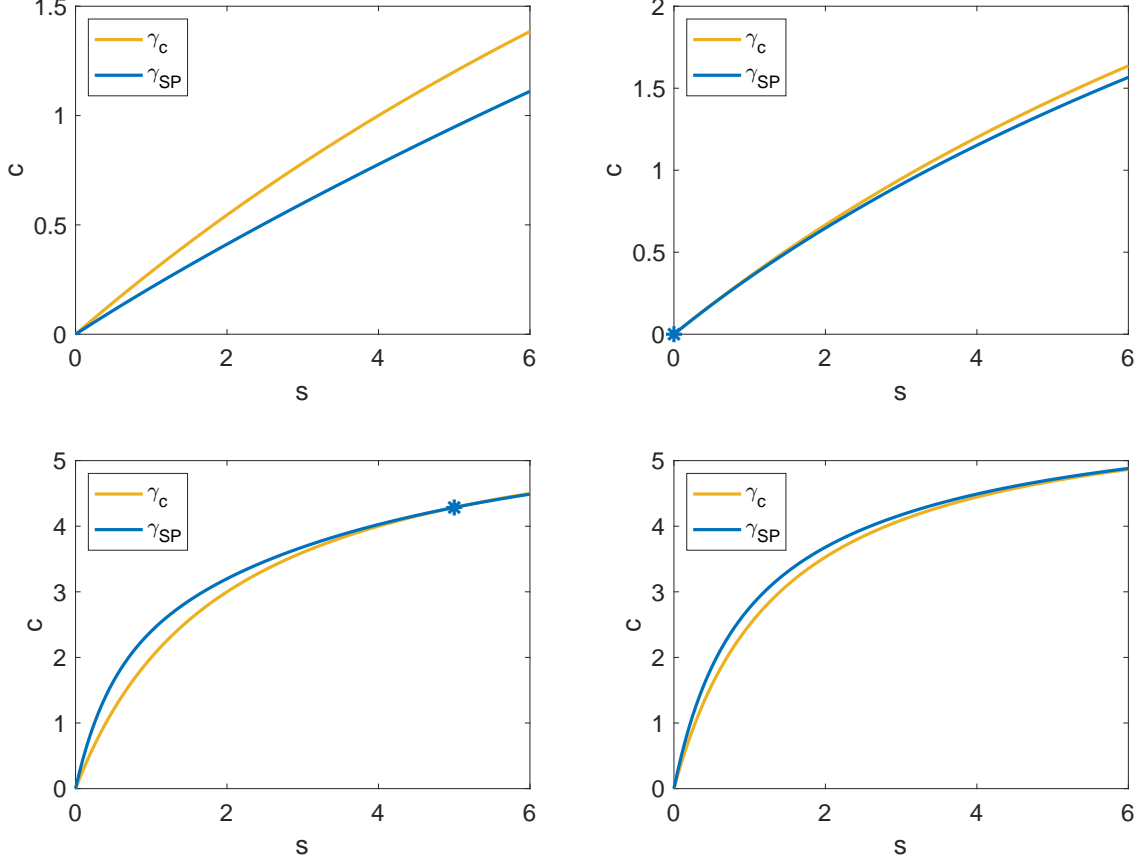


Figure 4: The slow product QSS curve γ_{SP} lies above the horizontal nullcline γ_c for $s < s^*$ (56) in the phase plane. **Top Left** ($k_2 > e_0 k_1$): $k_1 = 0.1$, $k_2 = 1$, $k_{-1} = 1$, $e_0 = 6$, $s^* = -4$. **Top Right** ($k_2 = e_0 k_1$): $k_1 = 0.1$, $k_2 = 0.6$, $k_{-1} = 1$, $e_0 = 6$, $s^* = 0$. **Bottom Left** ($k_2 < e_0 k_1$): $k_1 = 1$, $k_2 = 1$, $k_{-1} = 1$, $e_0 = 6$, $s^* = 5$. **Bottom Right** ($k_2 < e_0 k_1$): $k_1 = 1$, $k_2 = 0.4$, $k_{-1} = 1$, $e_0 = 6$, $s^* = 14$.

Do solutions cross $\gamma_{SP}(s)$ after crossing $\gamma_c(s)$ under any parametric conditions? If so, can we locate the slow manifold more precisely?

Numerical evidence suggests this is possible, with solutions lying closer to the slow product QSS curve in the steady-state regime (see Figure 5). Interestingly, the parametric conditions for this also ensure the slow-product QSS reduction's dominance over the sQSS reduction, aligning with our overall goal.

Our main results establish the conditions for positive invariance of the set bordered by the graphs of $\gamma_{SP}(s)$ and $\gamma(s)$:

$$\Gamma_{SP} := \{(s, c) \in \mathbb{R}_{\geq 0}^2 : \gamma_{SP}(s) \leq c \leq \gamma(s)\}, \quad (58)$$

and show that all solutions eventually cross $\gamma_{SP}(s)$ under those conditions.

Theorem 3. For a solution $(s, c)(t)$ to (2) with initial conditions $(s, c)(0) = (s_0, 0)$. If $e_0 < 8K_S$, then there exists a $t_{\text{cross_sp}} > 0$ at which the trajectory crosses $\gamma_{SP}(s)$, and

$$(s, c)(t) \in \Gamma_{SP}, \quad \forall t \geq t_{\text{cross_sp}}. \quad (59)$$

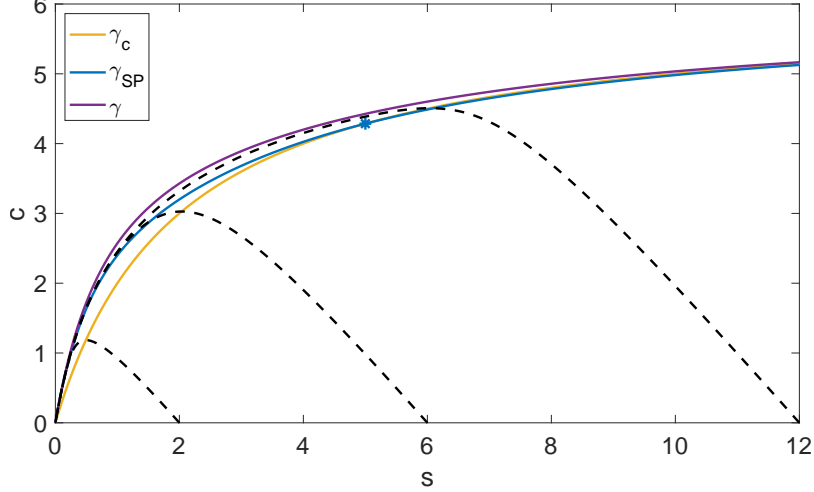


Figure 5: **The region between the slow product QSS curve $\gamma_{SP}(s)$ and the curve $\gamma(s)$ is a trapping region for solutions in the phase plane when $e_0 < 8K_S$.** The intersection point of γ_{SP} and γ_c , s^* , is denoted by the blue star. The numerical solutions to the mass action equations (1) for several initial conditions are denoted by black dashed lines. $s_0 \in \{2, 6, 12\}$, $c_0 = 0$, $e_0 = 6$, $k_1 = 1$, $k_{-1} = 1$, $k_2 = 1$.

Proof. To establish positive invariance, we show that the vector field at the boundary curve Γ_{SP} points towards Γ_{SP} when $e_0 < 8K_S$:

$$\dot{c}(s, \gamma_{SP}(s)) - \gamma'_{SP}(s)\dot{s}(s, \gamma_{SP}(s)) > 0 \quad (60)$$

See [Appendix C](#) for details. Combining this with (40a) ensures solutions entering Γ_{SP} remain within.

We also show that solutions beginning outside Γ_{SP} eventually enter it. In contradiction, assume that a solution starting at $(s_0, 0)$ converges to the stationary point $(0, 0)$ without entering Γ_{SP} . Then, the slope of the tangent to $c = \gamma_{SP}(s)$ at $s = 0$ should be greater than m (29). However, we show that

$$\gamma'_{SP}(0) < m \quad (61)$$

always holds, where:

$$\gamma'_{SP}(0) = \frac{k_1 e_0}{k_{-1}} - \frac{k_2 e_0}{k_{-1}(K_S + e_0)}. \quad (62)$$

When $e_0 < K$, $\gamma'_{SP}(0) < \gamma'_c(0)$ holds, and Theorem 2 implies $\gamma'_c(0) < m$, demonstrating $\gamma'_{SP}(0) < m$. For $e_0 > K$, see [Appendix D](#) for proof of (61). Thus, our assumption is false, and a $t_{\text{cross_sp}} > 0$ exists when the trajectory crosses $\gamma_{SP}(s)$. The proof is complete by combining the two arguments. \square

The primary benefit of establishing the positive invariance of Γ_{SP} is that it allows for a more precise localization of the slow manifold.

Theorem 4. If $e_0 < 8K_S$, then for the differential equation (23), Γ_{SP} is a positively invariant, narrowing anti-funnel within which there exists a unique slow manifold, S_0^ε .

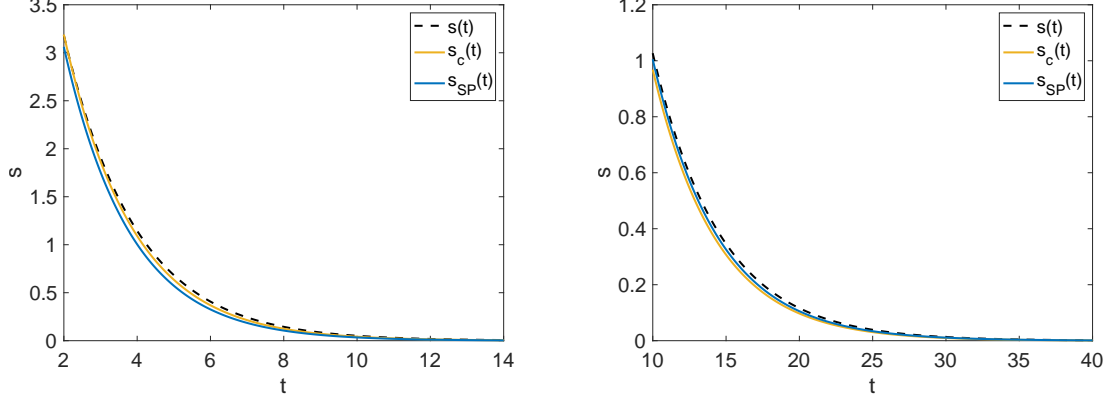


Figure 6: **The condition $e_0 < K$ ensures that the sQSSA provides a better approximation than the slow product QSSA under the Reich-Sel'kov condition.** $e_0 \ll K_M$ is satisfied in both panels. **Left ($e_0 < K$):** $s_0 = 9$, $c_0 = 0$, $e_0 = 6$, $k_1 = 1$, $k_{-1} = 100$, $k_2 = 10$. **Right ($e_0 > K$):** $s_0 = 9$, $c_0 = 0$, $e_0 = 6$, $k_1 = 1$, $k_{-1} = 100$, $k_2 = 4$. Substrate depletion over time is shown in both panels. The numerical solution to the mass action equations (1) is denoted by black dashed lines. $s_c(t)$ is the numerical solution to (16) and $s_{SP}(t)$ is the numerical solution to (17).

Proof. Inequality (60) ensures $c = \gamma_{SP}(s)$ is a strong upper fence for (23) when $e_0 < 8K_S$. It is verifiable that $\gamma(s) > \gamma_{SP}(s)$ for $s > 0$ and:

$$\lim_{s \rightarrow \infty} |\gamma(s) - \gamma_{SP}(s)| = 0 \quad (63)$$

implying Γ_{SP} (39) is a narrowing anti-funnel for $e_0 < 8K_S$. Further,

$$\frac{\partial f}{\partial c}(c, s) \geq 0 \quad (64)$$

in Γ_{SP} , and the claim follows from Theorem 1. \square

The slow manifold is contained within Γ_{SP} when $e_0 < 8K_S$. While this condition might seem restrictive, it connects directly to the sQSSA's validity analysis. We show that the slow manifold lies closer to the slow product QSS curve than the sQSS curve when $e_0 < 8K_S$. The remaining task is to analyze the implications of this location.

5.1. Revisiting the Reich-Sel'kov Condition

The Reich-Sel'kov qualifier ensures the sQSS reduction's accuracy, as validated in Section 4 using the novel anti-funnel (2). Our analysis shows that the sQSSA is the best known approximation to the slow manifold under most parametric scenarios. For instance, recall the intersection point (56). When $e_0 < K$, the intersection is inconsequential. Consequently, when the Reich-Sel'kov condition $e_0 \ll K_M$ is combined with $e_0 < K$, the sQSSA is the predominant approximation.

What happens when $e_0 \ll K_M$, $e_0 \ll K_S$ (ensuring $e_0 < 8K_S$), but $e_0 > K$? Theorem 3 implies that trajectories lie closer to γ_{SP} than to γ_c for a significant portion of the slow dynamics (see FIGURE 5), and therefore

$$-\frac{k_2 e_0 s}{K_M + s} \leq -\frac{k_2 e_0 s (K_S + s)}{K_S e_0 + (K_S + s)^2} \leq \dot{s} \leq -\frac{k_2 e_0 s (K_M + s)}{K_M e_0 + (K_M + s)^2} \quad (65)$$

after the trajectories cross γ_{SP} and $s \leq s^*$. Moreover, we know that the slope m of the linear approximation is greater than the slope of the tangent to γ_{SP} at the origin (61) and $\gamma'_{SP}(0) > \gamma'_c(0)$ whenever $e_0 > K$. Thus, the approximation errors near the stationary point follow:

$$m - \gamma'_{SP}(0) < m - \gamma'_c(0) \quad (66)$$

when $e_0 > K$. Consequently, complementing the Reich-Sel'kov condition with the stronger condition $e_0 < K$ is necessary to guarantee that the sQSS is indeed the predominant quasi-steady-state approximation of the MM reaction mechanism, and this may be relevant in the context of the inverse problem where parameters are estimated at low substrate concentration [3]: If $e_0 > K$, using the slow product QSS variety as an approximation for small s is beneficial. FIGURE 6 illustrates the numerical substrate depletion curves. The restrictive condition $e_0 < K$ is necessary to ensure the sQSS most accurately approximates the MM dynamics for small substrate concentrations.

6. Discussion

This work addresses a critical gap in the understanding of the quasi-steady-state approximation for the MM reaction mechanism. While the sQSSA is a widely used tool in enzyme kinetics, the precise conditions for its validity have remained a topic of ongoing investigation. We conducted a thorough phase-plane analysis of the MM mass-action kinetics using the theory of fences and anti-funnels, a powerful technique for analyzing the long-time behavior of dynamical systems.

Our analysis led to the identification of new positively invariant sets that contain the slow manifold, S_0^ε , in the substrate-complex phase plane. These sets provide valuable insights into the dynamics of the system and allow for a more precise characterization of the sQSSA's accuracy. As a result, we obtained improved bounds on the estimation error of various QSS approximations, including the standard, reverse, and slow product formation approximations, in the slow regime.

Significantly, we have demonstrated that the commonly accepted qualifier for the validity of the sQSSA, the Reich-Sel'kov condition ($e_0 \ll K_M$), does not guarantee that the sQSSA is the predominant reduction. Predominance necessitates a more restrictive condition

$$e_0 \ll K, \quad (67)$$

where K is the Van Slyke-Cullen constant. This finding challenges the traditional understanding of the sQSSA's validity and highlights the importance of considering both accuracy and predominance when evaluating QSS approximations.

It is important to note that our analysis primarily focused on the approximation error in the slow regime, specifically the error between the Fenichel reduction and the actual flow on the slow manifold, S_0^ε . However, two primary sources of error contribute to the overall accuracy of approximate solutions to singularly perturbed ODEs. The first is the error in approximating the flow on the slow manifold itself, as addressed in our analysis. The second is the error in approximating the trajectory's approach to the slow manifold, including timescale estimates such as t_{cross} , which demarcates the intersection of trajectories with pertinent QSS varieties. This latter source of error is generally more challenging to

analyze. Although some progress has been made in this area (see Eilertsen et al. [13]), further exploration and improvement is required.

Our findings have broader implications for the application of QSS approximations in various fields. By providing a more refined understanding of the sQSSA's validity, our work can guide researchers in selecting the most appropriate and accurate reduction for their specific needs. This is particularly crucial in areas such as quantitative biology and pharmacology, where accurate model reduction is essential for understanding complex biological processes and designing effective therapeutic interventions.

Future research could extend our analysis by considering more complex reaction mechanisms or incorporating additional factors that might influence the sQSSA's validity. Further investigation of the error associated with the trajectory's approach to the slow manifold is also warranted. By addressing these open questions, we can continue to refine our understanding of QSS approximations and enhance their utility in diverse scientific disciplines.

Acknowledgments

KS is supported by a research fellowship from the College of Science at the University of Notre Dame.

Appendices

These appendices provide supplementary information to enhance the understanding of the main text. The appendices include a synopsis of the theory of fences, funnels, and anti-funnels, as well as detailed calculations and proofs for key results presented in the paper.

Appendix A. Synopsis of the theory of Fences, funnels and antifunnels

This section highlights the notation of fences and anti-funnels within the context of the Michaelis-Menten system.

In general, an anti-funnel is the region above an upper fence and below a lower fence in a two-dimensional phase space. Typically, anti-funnels (or funnels) are visualized with the independent variable increasing from left to right. The vector field points outwards at the fences of an anti-funnel, while it points inwards at the fences of a funnel. Consequently, solutions generally leave anti-funnels. The anti-funnel theory implies that all but one solution eventually leave a narrowing anti-funnel [see 23, Chapter 1]). This property makes fences and anti-funnels useful for identifying a unique, exceptional solution that remains within the anti-funnel.

In the context of our work on the Michaelis-Menten system, the substrate concentration, s , decreases over time, with $s(0) = s_0$ and $s(t) \rightarrow 0$ as $t \rightarrow \infty$. In the (s, c) phase-plane, solution trajectories start at the substrate axis and move from right to left with respect to the s -axis. Thus, the vector field always has a negative component in the s -direction.

Despite this difference in directionality, the concept of anti-funnels remains applicable. The vector field can still point inwards at the anti-funnel fences in the (s, c) coordinate system as we move from right to left, while satisfying the conditions in Definition 1. Consequently, solution trajectories can enter the anti-funnels defined in the paper.

It is important to remember the nomenclature of upper and lower fences in this context. The slow manifold lies above the upper fence and below the lower fence in the phase plane.

Appendix B. Γ_0 is a positively invariant set for solutions in the phase plane

This section provides the detailed calculations to prove inequality (40a), which establishes the positive invariance of the set Γ_0 .

We begin by evaluating the dynamics at the curve $c = \gamma(s)$:

$$\dot{s}(s, \gamma(s)) = -k_1 e_0 s + k_1 (K_S + s) \gamma(s), \quad (\text{B.1a})$$

$$= -k_1 e_0 s + k_1 (K_S + s) \left(\frac{e_0 s}{K_S + s} - \frac{k_2 e_0 s (K_M + s)}{k_1 (K_S + s) (K_M e_0 + (K_M + s)^2)} \right), \quad (\text{B.1b})$$

$$= -\frac{k_2 e_0 s (K_M + s)}{K_M e_0 + (K_M + s)^2}, \quad (\text{B.1c})$$

and

$$\dot{c}(s, \gamma(s)) = k_1 e_0 s - k_1 (K_M + s) \gamma(s), \quad (\text{B.2a})$$

$$= k_1 e_0 s - k_1 (K_M + s) \left(\frac{e_0 s}{K_S + s} - \frac{k_2 e_0 s (K_M + s)}{k_1 (K_S + s) (K_M e_0 + (K_M + s)^2)} \right), \quad (\text{B.2b})$$

$$= -\frac{k_2 e_0 s}{K_S + s} + \frac{k_2 e_0 s (K_M + s)^2}{(K_S + s) (K_M e_0 + (K_M + s)^2)}. \quad (\text{B.2c})$$

The derivative of $\gamma(s)$ is:

$$\gamma'(s) = \frac{K_S e_0}{(K_S + s)^2} - \frac{k_2 K_S e_0 (K_M + s)}{k_1 (K_S + s)^2 (K_M e_0 + (K_M + s)^2)} \quad (\text{B.3})$$

$$- \frac{k_2 e_0 s}{k_1 (K_S + s) (K_M e_0 + (K_M + s)^2)} + \frac{2k_2 e_0 s (K_M + s)^2}{k_1 (K_S + s) (K_M e_0 + (K_M + s)^2)^2}. \quad (\text{B.4})$$

The required expression at $c = \gamma(s)$ is:

$$\dot{c} - \gamma'(s) \dot{s} = -\frac{k_2 e_0 s}{K_S + s} + \frac{k_2 e_0 s (K_M + s)^2}{(K_S + s) (K_M e_0 + (K_M + s)^2)} + \frac{k_2 e_0 s (K_M + s)}{K_M e_0 + (K_M + s)^2} \gamma'(s), \quad (\text{B.5a})$$

$$= -\frac{k_2 e_0 s}{(K_S + s) (K_M e_0 + (K_M + s)^2)} (K_M e_0 - (K_M + s) (K_S + s) \gamma'(s)). \quad (\text{B.5b})$$

To prove inequality (40a), we need to show that $\delta(s) = K_M e_0 - (K_M + s) (K_S + s) \gamma'(s) > 0$. This also proves that $\gamma(s)$ is a lower fence. Substituting $\gamma'(s)$ and simplifying, we obtain:

$$\begin{aligned} \delta(s) &= K_M e_0 - \frac{K_S e_0 (K_M + s)}{(K_S + s)} + \frac{k_2 K_S e_0 (K_M + s)^2}{k_1 (K_S + s) (K_M e_0 + (K_M + s)^2)} \\ &\quad + \frac{k_2 e_0 s (K_M + s)}{k_1 (K_M e_0 + (K_M + s)^2)} - \frac{2k_2 e_0 s (K_M + s)^3}{k_1 (K_M e_0 + (K_M + s)^2)^2}, \\ &= \frac{k_2 e_0}{k_1 (K_S + s) (K_M e_0 + (K_M + s)^2)^2} \left((K_M e_0 + (K_M + s)^2)^2 \right. \\ &\quad \left. + K_S (K_M + s)^2 (K_M e_0 + (K_M + s)^2) \right. \\ &\quad \left. + (K_M + s) (K_S + s) (K_M e_0 + (K_M + s)^2) s - 2(K_M + s)^3 (K_S + s) s \right). \end{aligned}$$

Expanding the first term in the expression,

$$\begin{aligned} \delta(s) &= \frac{k_2 e_0}{k_1 (K_S + s) (K_M e_0 + (K_M + s)^2)^2} \left((K_M e_0)^2 s + 2(K_M e_0) (K_M + s)^2 s + (K_M + s)^4 s \right. \\ &\quad \left. + K_S (K_M + s)^2 (K_M e_0 + (K_M + s)^2) \right. \\ &\quad \left. + (K_M + s) (K_S + s) (K_M e_0 + (K_M + s)^2) s - 2(K_M + s)^3 (K_S + s) s \right), \\ &= \frac{k_2 e_0}{k_1 (K_S + s) (K_M e_0 + (K_M + s)^2)^2} \left((K_M e_0)^2 s + 2(K_M e_0) (K_M + s)^2 s \right. \\ &\quad \left. + (k_2/k_1) (K_M + s)^3 s + K_S (K_M + s)^2 (K_M e_0 + (K_M + s)^2) \right. \\ &\quad \left. + K_M e_0 (K_M + s) (K_S + s) s \right), \end{aligned}$$

This expression is a sum of positive terms, proving inequality (40a).

For inequality (40b), a straightforward calculation at $c = \gamma_c(s)$ gives:

$$\dot{c} - \gamma'_c(s)\dot{s} = 0 + \left(\frac{K_M e_0}{(K_M + s)^2} \right) \left(\frac{k_2 e_0 s}{K_M + s} \right)$$

which is always positive for $s > 0$. Thus, Γ_0 is a positively invariant region.

Appendix C. Positive invariance of Γ_{SP} when $e_0 < 8K_S$

This section provides the detailed calculations to prove inequality (60), which establishes the positive invariance of the set γ_{SP} when $e_0 < 8K_S$.

We first compute the differential terms at γ_{SP} :

$$\dot{c}(s, \gamma_{SP}(s)) = k_1 e_0 s - k_1 (K_M + s) \gamma_{SP}(s), \quad (\text{C.1a})$$

$$= k_1 e_0 s - k_1 e_0 s \frac{(K_M + s)}{(K_S + s)} + \frac{k_2 e_0 s (K_M + s)}{K_S e_0 + (K_S + s)^2}, \quad (\text{C.1b})$$

$$= -\frac{k_2 e_0 s}{(K_S + s)} + \frac{k_2 e_0 (K_M + s) s}{K_S e_0 + (K_S + s)^2}, \quad (\text{C.1c})$$

and

$$\dot{s}(s, \gamma_{SP}(s)) = -k_1 e_0 s + k_1 (K_S + s) \gamma_{SP}(s), \quad (\text{C.2a})$$

$$= -\frac{k_2 e_0 (K_S + s) s}{K_S e_0 + (K_S + s)^2}. \quad (\text{C.2b})$$

The expression at $c = \gamma_{SP}(s)$ is:

$$\dot{c} - \gamma'_{SP}(s)\dot{s} = -\frac{k_2 e_0 s}{(K_S + s)} + \frac{k_2 e_0 (K_M + s) s}{K_S e_0 + (K_S + s)^2} + \frac{k_2 e_0 (K_S + s) s}{K_S e_0 + (K_S + s)^2} \gamma'_{SP}(s), \quad (\text{C.3a})$$

$$= \frac{k_2 e_0 s}{(K_S + s)(K_S e_0 + (K_S + s)^2)} \left(-(K_S e_0 + (K_S + s)^2) + \right. \quad (\text{C.3b})$$

$$\left. (K_M + s)(K_S + s) + (K_S + s)^2 \gamma'_{SP}(s) \right) \quad (\text{C.3c})$$

Proving inequality (60) simplifies to showing:

$$-(K_S e_0 + (K_S + s)^2) + (K_M + s)(K_S + s) + (K_S + s)^2 \gamma'_{SP}(s) > 0. \quad (\text{C.4})$$

This also proves that $\gamma_{SP}(s)$ is an upper fence. Substituting $\gamma'_{SP}(s)$:

$$\gamma'_{SP}(s) = \frac{K_S e_0}{(K_S + s)^2} - \frac{k_2 e_0}{k_1 (K_S e_0 + (K_S + s)^2)} + \frac{2k_2 e_0 (K_S + s) s}{k_1 (K_S e_0 + (K_S + s)^2)^2}, \quad (\text{C.5a})$$

and simplifying, we obtain:

$$\frac{k_2}{k_1} (K_S + s) - \frac{k_2 e_0 (K_S + s)^2}{k_1 (K_S e_0 + (K_S + s)^2)} + \frac{2k_2 e_0 (K_S + s)^3 s}{k_1 (K_S e_0 + (K_S + s)^2)^2} \quad (\text{C.6})$$

which is positive for $e_0 < 8K_S$. To show this, we further simplify the inequality to:

$$(K_S + s)^4 + e_0(K_S + s)^3 - K_S e_0^2 s > 0, \quad (\text{C.7a})$$

$$1 + \frac{e_0}{(K_S + s)} - \frac{K_S e_0^2 s}{(K_S + s)^4} > 0. \quad (\text{C.7b})$$

Substituting $e_0 = \eta K_S$ and introducing $x = K_S/(K_S + s)$, we get:

$$1 + \frac{e_0}{(K_S + s)} - \frac{K_S e_0^2 s}{(K_S + s)^4} = 1 + \eta x - \eta^2 x^3 (1 - x) = \eta^2 x^4 - \eta^2 x^3 + \eta x + 1. \quad (\text{C.8})$$

We want to show that $\eta^2 x^4 - \eta^2 x^3 + \eta x + 1 > 0$ for $\eta < 8$. Dividing by η^2 and factoring the quartic function, we get:

$$x^4 - x^3 + \frac{1}{\eta} x + \frac{1}{\eta^2} = \left(x^2 + \bar{\eta}_+ x - \frac{1}{\eta} \right) \left(x^2 + \bar{\eta}_- x - \frac{1}{\eta} \right) \quad (\text{C.9})$$

where

$$\bar{\eta}_\pm = -\frac{1}{2} \pm \frac{1}{2} \sqrt{\frac{\eta - 8}{\eta}}.$$

This quartic function has no real roots when $\eta < 8$ and remains positive. It has 2 real repeated roots for $\eta = 8$ and 4 real roots when $\eta > 8$. This completes the proof for the first part of Theorem 3.

Appendix D. Solutions approach the origin at a slope greater than $\gamma'_{SP}(0)$.

This section provides the details to prove the inequality:

$$m - \gamma'_{SP}(0) > 0 \quad (\text{D.1})$$

when $k_2 < k_1 e_0$, completing the proof for Theorem 3.

Recall:

$$m = \frac{1}{2k_{-1}} \left(-k_{-1} - k_2 + k_1 e_0 + \sqrt{(k_{-1} + k_2 + k_1 e_0)^2 - 4k_1 k_2 e_0} \right) \quad (\text{D.2})$$

and

$$\gamma'_{SP}(0) = \frac{k_1 e_0}{k_{-1}} - \frac{k_2 k_1 e_0}{k_{-1}(k_1 e_0 + k_{-1})}. \quad (\text{D.3})$$

Therefore, $m - \gamma'_{SP}(0)$ is:

$$m - \gamma'_{SP}(0) = \frac{-(k_{-1} + k_2 + k_1 e_0)}{2k_{-1}} + \frac{k_2 k_1 e_0}{k_{-1}(k_1 e_0 + k_{-1})} \quad (\text{D.4a})$$

$$+ \frac{1}{2k_{-1}} \sqrt{(k_{-1} + k_2 + k_1 e_0)^2 - 4k_1 k_2 e_0}, \quad (\text{D.4b})$$

$$= \frac{-(k_{-1} + k_1 e_0)}{2k_{-1}} + \frac{k_2(k_1 e_0 - k_{-1})}{2k_{-1}(k_1 e_0 + k_{-1})} + \frac{1}{2k_{-1}} \sqrt{(k_{-1} + k_2 + k_1 e_0)^2 - 4k_1 k_2 e_0}, \quad (\text{D.4c})$$

$$= \frac{-(k_{-1} + k_1 e_0)}{2k_{-1}} + \frac{k_2(k_1 e_0 - k_{-1})}{2k_{-1}(k_1 e_0 + k_{-1})} \quad (\text{D.4d})$$

$$+ \frac{1}{2k_{-1}} \sqrt{(k_{-1} + k_1 e_0)^2 + k_2^2 + 2k_2 k_{-1} - 2k_1 k_2 e_0}. \quad (\text{D.4e})$$

Simplifying this expression, we want to show:

$$\frac{-(k_{-1} + k_1 e_0)}{2k_{-1}} + \frac{k_2(k_1 e_0 - k_{-1})}{2k_{-1}(k_1 e_0 + k_{-1})} + \frac{1}{2k_{-1}} \sqrt{(k_{-1} + k_1 e_0)^2 + k_2^2 - 2k_2(k_1 e_0 - k_{-1})} > 0 \quad (\text{D.5})$$

or

$$\frac{1}{2k_{-1}} \sqrt{(k_{-1} + k_1 e_0)^2 + k_2^2 - 2k_2(k_1 e_0 - k_{-1})} > \frac{(k_{-1} + k_1 e_0)}{2k_{-1}} - \frac{k_2(k_1 e_0 - k_{-1})}{2k_{-1}(k_1 e_0 + k_{-1})}. \quad (\text{D.6})$$

The above expression is equivalent to:

$$(k_1 e_0 + k_{-1}) \sqrt{(k_{-1} + k_1 e_0)^2 + k_2^2 - 2k_2(k_1 e_0 - k_{-1})} > (k_1 e_0 + k_{-1})^2 - k_2(k_1 e_0 - k_{-1}). \quad (\text{D.7})$$

When $k_2 < k_1 e_0$, both sides are positive. Thus, we can prove that the above inequality is true by showing that the corresponding squared terms satisfy the same inequality. In simpler words, if $a, b > 0$ and $a^2 > b^2$, then $a > b$. Squaring both sides and simplifying, we can verify that:

$$(k_1 e_0 + k_{-1})^2 ((k_{-1} + k_1 e_0)^2 + k_2^2 - 2k_2(k_1 e_0 - k_{-1})) > (k_1 e_0 + k_{-1})^4 + k_2^2(k_1 e_0 - k_{-1})^2 - 2k_2(k_1 e_0 - k_{-1})(k_1 e_0 + k_{-1})^2. \quad (\text{D.8})$$

Hence, the inequality $m - \gamma'_{SP}(0) > 0$ holds when $k_2 < k_1 e_0$.

Appendix E. Singular perturbation analysis of large k_{-1}

In perturbation form, the Michaelis-Menten mass action equations with large k_{-1} is

$$\dot{s} = -k_1(e_0 - c)s + \varepsilon^{-1} \widehat{k}_{-1} c, \quad (\text{E.1a})$$

$$\dot{c} = k_1(e_0 - c)s - k_2 c - \varepsilon^{-1} \widehat{k}_{-1} c, \quad (\text{E.1b})$$

which admits the corresponding layer problem:

$$\dot{s} = \varepsilon^{-1} \widehat{k}_{-1} c, \quad (\text{E.2a})$$

$$\dot{c} = -\varepsilon^{-1} \widehat{k}_{-1} c. \quad (\text{E.2b})$$

The critical manifold is therefore s -axis and is normally hyperbolic and attracting. The projection matrix, π^s , is given by

$$\pi^s = \begin{pmatrix} 1 & 1 \\ 0 & 0 \end{pmatrix}. \quad (\text{E.3})$$

The Fenichel reduction is therefore

$$\begin{pmatrix} \dot{s} \\ \dot{c} \end{pmatrix} = \begin{pmatrix} 1 & 1 \\ 0 & 0 \end{pmatrix} \cdot \begin{pmatrix} -k_1(e_0 - c)s + \varepsilon^{-1} \widehat{k}_{-1} c \\ k_1(e_0 - c)s - k_2 c - \varepsilon^{-1} \widehat{k}_{-1} c \end{pmatrix} \Big|_{c=0} = \begin{pmatrix} 0 \\ 0 \end{pmatrix} \quad (\text{E.4})$$

which is trivial. Thus, one must appeal to higher-order terms in order to recover a non-trivial QSSA.

References

- [1] L. Michaelis, M. L. Menten, Die Kinetik der Invertinwirkung, *Biochem. Z.* 49 (1913) 333–369.
- [2] S. Schnell, P. K. Maini, A century of enzyme kinetics. Reliability of the K_M and v_{\max} estimates, *Comments Theor. Biol.* 8 (2003) 169–187.
- [3] W. Stroberg, S. Schnell, On the estimation errors of K_M and v from time-course experiments using the michaelis–menten equation, *Biophys. Chem.* 219 (2016) 17–27.
- [4] B. Choi, G. A. Rempala, J. K. Kim, Beyond the Michaelis–Menten equation: Accurate and efficient estimation of enzyme kinetic parameters, *Sci. Rep.* 7 (2017) 17018.
- [5] S. Schnell, Validity of the Michaelis–Menten equation – steady-state or reactant stationary assumption: that is the question, *FEBS J.* 281 (2014) 464–472.
- [6] A. Goeke, S. Walcher, E. Zerz, Determining “small parameters” for quasi-steady state, *J. Differential Equations* 259 (2015) 1149–1180.
- [7] J. Eilertsen, S. Schnell, S. Walcher, The unreasonable effectiveness of the total quasi-steady state approximation, and its limitations, *J. Theor. Biol.* 583 (2024) Paper No. 111770.
- [8] H. G. Kaper, T. J. Kaper, Asymptotic analysis of two reduction methods for systems of chemical reactions, *Physica D* 165 (2002) 66–93.
- [9] G. Hek, Geometric singular perturbation theory in biological practice, *J. Math. Biol.* 60 (2010) 347–386.
- [10] C. K. R. T. Jones, Geometric singular perturbation theory, in: *Dynamical systems (Montecatini Terme, 1994)*, volume 1609 of *Lecture Notes in Math.*, Springer, Berlin, 1995, pp. 44–118.
- [11] M. Wechselberger, Geometric singular perturbation theory beyond the standard form, volume 6 of *Frontiers in Applied Dynamical Systems: Reviews and Tutorials*, Springer, Cham, 2020.
- [12] J. Eilertsen, S. Schnell, S. Walcher, Natural parameter conditions for singular perturbations of chemical and biochemical reaction networks, *Bull. Math. Biol.* 85 (2023) Paper No. 48, 75.
- [13] J. Eilertsen, S. Schnell, S. Walcher, Rigorous estimates for the quasi-steady state approximation of the Michaelis–Menten reaction mechanism at low enzyme concentrations, *Nonlinear Anal. Real World Appl.* 78 (2024) Paper No. 104088, 27.
- [14] J. Reich, E. Sel’kov, Mathematical-analysis of metabolis networks, *FEBS Lett.* 43 (1974) S119–S127.

- [15] N. Fenichel, Persistence and smoothness of invariant manifolds for flows, *Indiana Univ. Math. J.* 21 (1971/72) 193–226.
- [16] N. Fenichel, Geometric singular perturbation theory for ordinary differential equations, *J. Differ. Equ.* 31 (1979) 53–98.
- [17] A. Goeke, S. Walcher, A constructive approach to quasi-steady state reductions, *J. Math. Chem.* 52 (2014) 2596–2626.
- [18] A. Goeke, S. Walcher, E. Zerz, Classical quasi-steady state reduction—a mathematical characterization, *Phys. D* 345 (2017) 11–26.
- [19] J. Eilertsen, S. Schnell, The quasi-steady-state approximations revisited: timescales, small parameters, singularities, and normal forms in enzyme kinetics, *Math. Biosci.* 325 (2020) Paper No. 108339.
- [20] H.-W. Kang, W. R. KhudaBukhsh, H. Koepl, G. A. Rempal a, Quasi-steady-state approximations derived from the stochastic model of enzyme kinetics, *Bull. Math. Biol.* 81 (2019) 1303–1336.
- [21] E. A. Mastny, E. L. Haseltine, J. B. Rawlings, Two classes of quasi-steady-state model reductions for stochastic kinetics, *J. Chem. Phys.* 127 (2007) 094106.
- [22] J. Eilertsen, K. Srivastava, S. Schnell, Stochastic enzyme kinetics and the quasi-steady-state reductions: application of the slow scale linear noise approximation à la Fenichel, *J. Math. Biol.* 85 (2022) Paper No. 3, 27.
- [23] J. H. Hubbard, B. H. West, Differential equations: A dynamical systems approach, volume 5 of *Texts in Applied Mathematics*, Springer-Verlag, New York, 1995. Ordinary differential equations, Corrected reprint of the 1991 edition.
- [24] M. S. Calder, D. Siegel, Properties of the Michaelis-Menten mechanism in phase space, *J. Math. Anal. Appl.* 339 (2008) 1044–1064.
- [25] L. Noethen, S. Walcher, Quasi-steady state in the Michaelis-Menten system, *Nonlinear Anal. Real World Appl.* 8 (2007) 1512–1535.
- [26] J. Eilertsen, S. Schnell, S. Walcher, On the anti-quasi-steady-state conditions of enzyme kinetics, *Math. Biosci.* 350 (2022) Paper No. 108870.
- [27] A. Kumar, K. Josić, Reduced models of networks of coupled enzymatic reactions, *J. Theoret. Biol.* 278 (2011) 87–106.
- [28] F. G. Heineken, H. M. Tsuchiya, R. Aris, On the mathematical status of the pseudo-steady hypothesis of biochemical kinetics, *Math. Biosci.* 1 (1967) 95–113.
- [29] L. A. Segel, M. Slemrod, The quasi-steady-state assumption: A case study in perturbation, *SIAM Rev.* 31 (1989) 446–477.
- [30] L. A. Segel, On the validity of the steady state assumption of enzyme kinetics, *Bull. Math. Biol.* 50 (1988) 579–593.